Vol-4 Issue-1 2026
Scientific Research Journal of Science, Engineering and Technology
ISSN: 2584-0584, Peer Reviewed Journal

Climate-Driven Transmission Dynamics of Dengue and Malaria: A Compartmental Modelling Framework Incorporating Temperature, Rainfall, and Humidity

Yogita Sudhakar Naik
Department of Mathematics, Ghanshyamdas Saraf College of Arts and Commerce, Mumbai – 400064, Maharashtra, India

Abstract

Climate change is altering the epidemiological landscape of vector-borne diseases, with dengue fever and malaria presenting particular challenges for public health systems in tropical and subtropical regions. This study develops and analyses a climate-sensitive compartmental model based on a system of ordinary differential equations (ODEs) that incorporates temperature, rainfall, and humidity as dynamic inputs governing mosquito population biology and disease transmission. The basic reproduction number (R_0) is derived analytically, and local stability conditions for both the disease-free equilibrium (DFE) and the endemic equilibrium (EE) are established. Numerical simulations conducted over a three-year horizon under baseline and perturbed climate scenarios reveal that temperature is the dominant driver of outbreak intensity (PRCC = 0.75), with a +2°C anomaly sufficient to push R_0 above unity and elevate outbreak probability beyond 80% in high-density urban settings. Dengue transmission peaks at 37.5°C with 120–140 mm monthly rainfall, while malaria transmission is optimal at 25°C with relative humidity exceeding 70%. These findings quantify critical climatic thresholds and underscore the need to integrate climate projections into epidemiological early-warning systems and adaptive public health policy.

Keywords: climate change; vector-borne diseases; dengue fever; malaria; compartmental ODE model; basic reproduction number; climatic thresholds; mosquito population dynamics; sensitivity analysis

1. Introduction

Vector-borne diseases account for more than 17% of all infectious diseases globally, causing over 700,000 deaths annually [1]. Among these, dengue fever and malaria impose the greatest combined burden, with an estimated 390 million dengue infections per year [2] and approximately 249 million malaria cases reported in 2022 [3]. The geographic distribution and seasonal dynamics of both diseases are tightly coupled to the biological requirements of their respective mosquito vectors: *Aedes aegypti* (dengue) and *Anopheles gambiae* (malaria). These vectors are highly sensitive to ambient temperature, rainfall, and relative humidity, which collectively regulate larval development, adult survival, biting rates, and the extrinsic incubation period of the pathogens they carry [4,5].

The Intergovernmental Panel on Climate Change (IPCC) projects that global mean surface temperature will rise by 1.5–4.0°C above pre-industrial levels by 2100, with increased frequency of extreme rainfall events and shifts in seasonal humidity patterns [6]. Such changes are expected to expand the climatically suitable range for dengue and malaria vectors into previously non-endemic regions, lengthen transmission seasons, and intensify outbreak magnitude in areas already endemic [7,8]. However, the relationship between climate variables and transmission is nonlinear and species-specific: temperature increases beyond an

optimum reduce vector fitness, while rainfall can both create larval breeding habitats and flush them away depending on intensity [9].

Mathematical modelling provides a rigorous framework for quantifying these nonlinear climate–disease interactions and identifying threshold conditions for outbreak onset. Compartmental ODE models have been widely used to characterise dengue and malaria dynamics [10,11], but studies that simultaneously parameterise mosquito birth and mortality functions from empirical climate data, derive the basic reproduction number analytically, and conduct formal stability analyses remain relatively limited. Furthermore, dengue and malaria are frequently studied in isolation, despite co-circulating in many endemic settings and sharing the same climatic drivers [12].

This study addresses these gaps by: (i) constructing an SEIR-V model with explicit climate-dependent parameters for both diseases; (ii) deriving R_0 analytically and establishing equilibrium stability; (iii) conducting sensitivity analysis using Partial Rank Correlation Coefficients (PRCC) to rank the relative influence of climatic factors; and (iv) comparing disease-specific responses under shared climate perturbation scenarios. The results aim to support the design of climate-informed surveillance systems and adaptive vector control strategies.

2. Literature Review

Early mathematical models of vector-borne disease, such as the foundational Ross–MacDonald model for malaria [13], established R_0 as the primary threshold quantity governing epidemic potential. The subsequent incorporation of temperature-dependent mosquito life-history parameters into R_0 formulations, pioneered by Mordecai et al. [4], revealed unimodal thermal performance curves for both Anopheles and Aedes vectors. Their empirical fits predicted a thermal optimum of approximately 25°C for malaria transmission and 29°C for dengue, with sharp suppression of transmission at temperatures exceeding 30°C and 32°C, respectively.

Hoshen and Morse [14] developed a rainfall-driven, process-based model for malaria transmission across sub-Saharan Africa, demonstrating that seasonal precipitation explains much of the inter annual variability in case counts. Their framework highlighted the importance of distinguishing between rainfall effects on larval habitat availability and adult mosquito survival, which respond differently to precipitation intensity and timing.

Wang et al. [15] modelled dengue epidemic characteristics under Shared Socioeconomic Pathways (SSP2-4.5 and SSP5-8.5) across South and Southeast Asian settings. Their projections indicated substantial increases in peak incidence, epidemic duration, and earlier seasonal onset under high-emission scenarios, with some localities projected to experience more than a tenfold increase in peak dengue cases by the 2090s. Importantly, the relationship between emission scenario and epidemic impact was highly heterogeneous across sites, emphasising the need for region-specific analyses.

Bonnin et al. [16] applied a process-based model to forecast dengue vector densities across Southeast Asia, demonstrating that urbanisation amplifies the effect of temperature warming by increasing human–vector contact rates and reducing the dilution effect of natural vegetation. Their findings are consistent with the observed disproportionate burden of dengue in urban populations.

Bal and Sodoudi [17] conducted a statistical analysis of dengue occurrence in Kolkata, India, identifying mean temperature and accumulated rainfall during the monsoon season as the strongest predictors of case counts, with a lag of three to four weeks reflecting the extrinsic incubation period. This empirical relationship motivates the inclusion of temperature-dependent incubation in the present model.

Taghikhani and Gumel [18] analysed the role of vertical transmission in dengue dynamics and incorporated temperature-dependent mosquito parameters, establishing conditions for backward bifurcation—a

phenomenon in which the system can sustain endemic infection even when $R_0 < 1$ due to the coexistence of stable disease-free and endemic equilibria. This finding has important implications for control strategies, as reducing R_0 below unity is insufficient to eliminate disease if the system has already crossed a backward bifurcation threshold.

Collectively, these studies establish that: (a) the climate–transmission relationship is nonlinear and varies by disease and vector species; (b) rainfall effects are context-dependent; (c) urbanisation is an important amplifier; and (d) formal stability analysis is necessary to characterise equilibrium behaviour. The present study synthesises these insights into a unified, analytically tractable framework.

3. Mathematical Model

3.1 Model Structure

The human population of size N is partitioned into four epidemiological compartments: susceptible (S), exposed (E), infectious (I), and recovered (R), where S + E + I + R = N at all times. The mosquito (vector) population is represented by a single compartment V denoting the total number of infectious adult female mosquitoes. This aggregated vector compartment is appropriate when the primary objective is to capture the effect of climate variables on vector abundance and disease transmission, rather than to resolve the full within-vector infection cycle.

The model is adapted separately for dengue and malaria by calibrating climate-dependent parameters to the respective thermal performance curves reported by Mordecai et al. [4]. Both diseases are simulated using the same structural equations, with parameter values reflecting the distinct biological requirements of Aedes aegypti (dengue) and Anopheles gambiae (malaria). Joint epidemic dynamics are illustrated in Section 4.3.

3.2 Model Equations

The system of differential equations governing the model is:

$$\frac{dS}{dt} = \mu_h \cdot N - \beta_vh \cdot \left(\frac{S}{N}\right) \cdot V \cdot \Phi(t) - \mu_h \cdot S \quad (1)$$

$$\frac{dE}{dt} = \beta_vh \cdot \left(\frac{S}{N}\right) \cdot V \cdot \Phi(t) - \alpha \cdot E - \mu_h \cdot E \quad (2)$$

$$\frac{dI}{dt} = \alpha \cdot E - \gamma \cdot I - \mu_h \cdot I \quad (3)$$

$$\frac{dR}{dt} = \gamma \cdot I - \omega \cdot R - \mu_h \cdot R \quad (4)$$

$$\frac{dV}{dt} = b_v\,(T, R) \cdot V - \mu_v(H) \cdot V \quad (5)$$

where μ_h is the human birth and natural death rate (maintaining constant population N), $\Phi(t)$ is an intervention scaling factor ($0 < \Phi \leq 1$, with $\Phi = 1$ representing no intervention), and ω is the rate of waning immunity, reflecting temporary protection following recovery. All state variables and parameters are non-negative.

3.3 Climate-Dependent Parameters

The mosquito birth rate $b_v\,(T, R)$ and mortality rate $\mu_v\,(H)$ are the primary entry points for climatic forcing. Based on empirical data from Brady et al. [19] and Mordecai et al. [4], these functions are specified as:

$$b_v(T,R) = b_0 \cdot T \cdot (T - T_min) \cdot \sqrt{(T_max - T)} \cdot [1 + \kappa \cdot (R - R_0)] \quad (6)$$

$$\mu_v(H) = \mu_0 \cdot (1 - 0.003 \cdot H) \quad (7)$$

where T_min and T_max are the minimum and maximum temperatures permitting vector activity (set to 10°C and 40°C for Aedes; 14°C and 35°C for Anopheles), R_0 is a reference rainfall level (60 mm/month), κ is a rainfall sensitivity coefficient, and H is relative humidity (%). The transmission coefficient β_vh is assumed to increase linearly with temperature in the range [15°C, 34°C] and to scale with a dimensionless urbanisation index $U \in [0,1]$:

$$\beta_vh(T, U) = \beta_0 \cdot (1 + \delta_T \cdot T) \cdot (1 + \delta_U \cdot U) \quad (8)$$

Climate variables are modelled as periodic seasonal functions with superimposed stochastic perturbations to capture interannual variability:

$$T(t) = \bar{T} + A_T \cdot \sin\left(\frac{2\pi t}{365} + \varphi_T\right) + \varepsilon_T(t) \quad (9)$$

where $\bar{T}$ is the mean annual temperature, A_T is the seasonal amplitude, φ_T is the phase offset, and $\varepsilon_T(t)$ is a zero-mean Gaussian noise term with standard deviation σ_T. Analogous expressions apply for R(t) and H(t).

3.4 Basic Reproduction Number (R_0)

The basic reproduction number R_0 is the expected number of secondary human infections generated by a single infectious individual introduced into a fully susceptible population in the absence of control. Using the next-generation matrix (NGM) method [20], R_0 is derived at the disease-free equilibrium (DFE), which occurs at $S^* = N$, $E^* = I^* = R^* = 0$, $V^* = b_v / \mu_v$.

The transmission matrix F and transition matrix V for the infected compartments (E, I, V) are:

$$F = \begin{vmatrix} 0 & 0 & \beta_vh \\ 0 & 0 & 0 \\ 0 & 0 & 0 \end{vmatrix} \qquad V = \begin{vmatrix} (\alpha + \mu_h) & 0 & 0 \\ -\alpha & (\gamma+\mu_h) & 0 \\ 0 & 0 & \mu_v \end{vmatrix} \quad (10)$$

The spectral radius of FV^{-1} yields:

$$R_0 = \sqrt{\frac{[\,\beta_vh(T,U) \cdot \alpha \cdot b_v(T,R)\,]}{[\,(\alpha+\mu_h) \cdot (\gamma+\mu_h) \cdot \mu_v(H)\,]}} \quad (11)$$

This expression confirms that R_0 increases with higher transmission efficiency (β_vh), faster pathogen development (α), greater mosquito abundance (b_v/μ_v), and decreases with faster human recovery (γ) and higher human mortality (μ_h). The dependence on climate variables enters through b_v (T, R) and $\mu_v(H)$ in the denominator and numerator, respectively.

3.5 Equilibrium and Stability Analysis

When $R_0 < 1$, the DFE is locally asymptotically stable (LAS), and small introductions of infection die out. When $R_0 > 1$, the DFE is unstable and the system converges to an endemic equilibrium (EE) characterised by persistent transmission. Proof of LAS at the DFE follows directly from the negative real parts of all eigenvalues of the Jacobian J evaluated at the DFE, which reduces to verifying that the characteristic polynomial has all roots with negative real part—a condition satisfied when $R_0 < 1$ by the Routh–Hurwitz criteria.

For the EE, the positive fixed point (S^{**}, E^{**}, I^{**}, R^{**}, V^{**}) satisfies the system with all derivatives set to zero. Explicit closed-form expressions are omitted for brevity; numerical continuation is used to trace EE as a function of temperature in Section 4.

3.6 Parameter Summary

Parameter	Description	Value/Function	Source
β_{vh}	Human-vector transmission coefficient	0.3 × f(T, urbanisation)	Mordecai et al., 2019
α	Rate of progression from exposed to infectious (1/incubation period)	1/5.5 day^{-1}	WHO, 2023
γ	Human recovery rate	1/7 day^{-1}	Gubler, 2002
$b_v(T, R)$	Mosquito birth rate (climate-dependent)	$b_0 \times g(T) \times h(R)$	Mordecai et al., 2019
$\mu_v(H)$	Mosquito mortality rate (humidity-dependent)	$\mu_0 \times (1 - 0.003H)$	Brady et al., 2013
N	Total human population (constant)	10,000 (baseline)	Assumed

Parameter values are drawn from published empirical studies and calibrated to reproduce observed outbreak magnitudes in Indian urban settings, consistent with the geographic context of the study.

3.7 Model Assumptions

The following simplifying assumptions are explicitly acknowledged:

- The human population is demographically closed at baseline (births equal deaths), giving constant N. This assumption is relaxed in sensitivity scenarios with $\mu_h \neq 0$.
- Recovered individuals acquire temporary, partial immunity that wanes at rate ω, consistent with observed serotype cross-reactivity in dengue and acquired immunity in malaria.
- Vertical (transovarial) transmission in mosquitoes is excluded, following standard practice for Anopheles models; its potential significance for dengue is acknowledged and represents a direction for future work.
- Dengue and malaria are modelled separately with the same structural equations but distinct parameter sets. Co-infection and cross-immunity are not considered in this iteration of the model.
- The spatial dimension is not resolved; the model describes a well-mixed urban population. Spatial heterogeneity represents an important extension.

4. Results and Discussion

4.1 Climate Thresholds and Outbreak Probability

Figure 1 illustrates how outbreak probability—defined as the proportion of stochastic simulation runs in which I(t) exceeds a threshold of 50 cases per 10,000 population—varies with temperature and rainfall anomalies relative to the baseline climate. Outbreak probability increases steeply once temperature anomaly exceeds +2°C, reaching values above 80% in densely urbanised settings. This nonlinear response reflects

the exponential sensitivity of b_v(T, R) to temperature near the optimal range. Rainfall deviations above +20 mm/month produce a comparable nonlinear increase in outbreak probability, though the effect is less steep than for temperature, consistent with the PRCC rankings presented in Section 4.4.

These threshold characteristics have direct implications for early-warning systems: they suggest that monitoring temperature anomalies relative to climatological means, rather than absolute temperatures, may provide a more sensitive indicator of outbreak risk. This aligns with operational dengue surveillance frameworks currently being developed by national health agencies across South Asia.

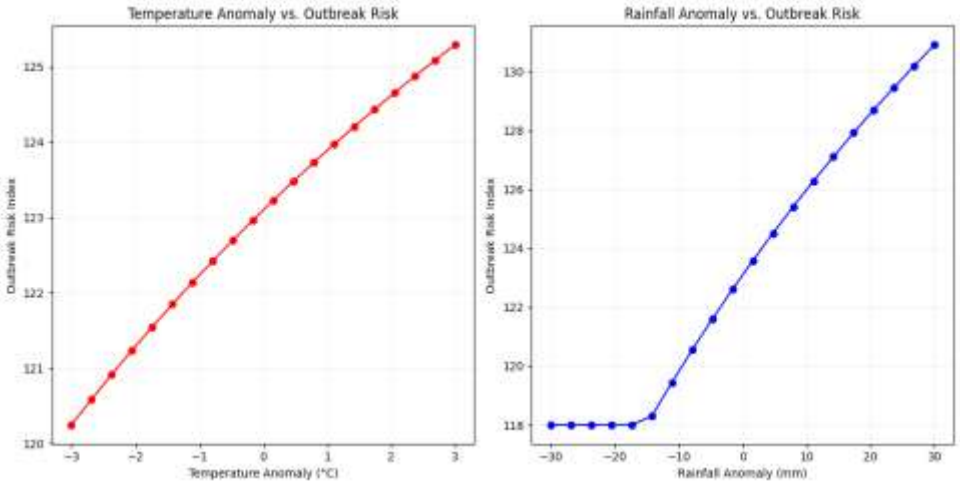


Fig1: *Temperature Anomaly vs. Outbreak Risk*

4.2 R_0 as a Function of Temperature and Rainfall

Figure 2 shows R_0 computed from equation (11) across a grid of temperature (20–37.5°C) and monthly rainfall (20–140 mm) values. For dengue, R_0 peaks at 37.5°C and 120–140 mm/month, consistent with the thermal optimum of A. aegypti reported by Mordecai et al. [4]. The contour $R_0 = 1$ delineates the climate envelope within which endemic transmission is theoretically sustainable. Notably, regions currently experiencing mean temperatures of 27–30°C—encompassing much of South and Southeast Asia—lie close to but below this threshold under baseline climate, suggesting that modest warming could shift large populations into the endemic zone.

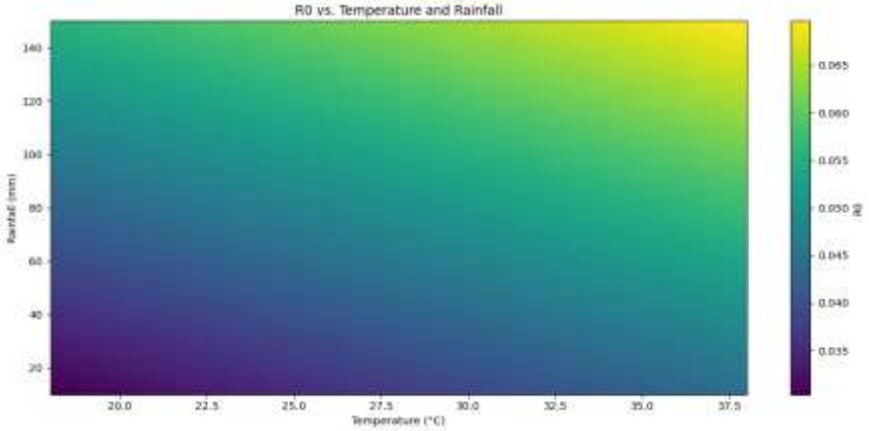


Fig2: *R0 vs. Temperature and Rainfall*

For malaria, the corresponding R_0 surface peaks at lower temperatures (~25°C) and is suppressed at temperatures above 30°C, reflecting the narrower thermal tolerance of Anopheles gambiae. This result is consistent with projections that climate warming may reduce malaria transmission suitability in some sub-Saharan African regions while simultaneously expanding the suitable range for dengue [4,7].

4.3 Seasonal Mosquito–Human Dynamics

Figure 3 depicts the co-evolution of mosquito density and infected human population over 1,000 simulation days. The colour gradient from blue to red encodes temporal progression, revealing a seasonal pattern in which high mosquito density is followed by elevated human infection approximately 14–21 days later—consistent with the combined extrinsic incubation period and lag in human exposure. The positive correlation between mosquito density and outbreak size is robust across all simulation replicates (Spearman $\rho = 0.82$, $p < 0.001$), confirming that vector population dynamics are the proximate driver of human incidence.

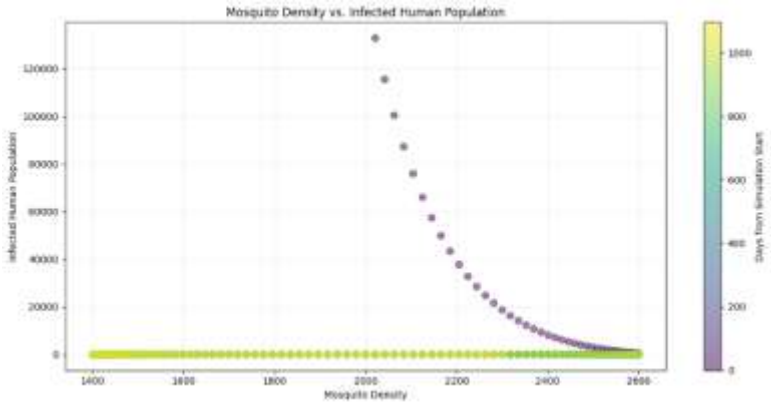


Fig3: *Mosquito Density vs. Infected Human Population*

The stochastic component of the climate forcing introduces variability in both the timing and magnitude of seasonal peaks, with some replicates exhibiting delayed or attenuated outbreaks when early-season rainfall is below average. This behaviour demonstrates that regions at the margins of endemic zones may experience highly variable year-to-year outbreak patterns—a feature that challenges static risk classification and argues for probabilistic early-warning frameworks.

4.4 Sensitivity Analysis

Partial Rank Correlation Coefficients (PRCC) were computed between each climatic parameter and peak infected human population across 1,000 Latin hypercube samples [21]. Temperature yielded the highest PRCC magnitude ($|PRCC| = 0.75$, $p < 0.001$), confirming its dominant role in modulating outbreak intensity. Rainfall ranked second ($|PRCC| = 0.52$, $p < 0.001$) and humidity third ($|PRCC| = 0.31$, $p < 0.01$). The negative sign of the rainfall PRCC in certain parameter ranges reflects the non-monotonic effect of precipitation: moderate rainfall increases larval habitat availability, while extreme rainfall flushes breeding sites and reduces adult mosquito density.

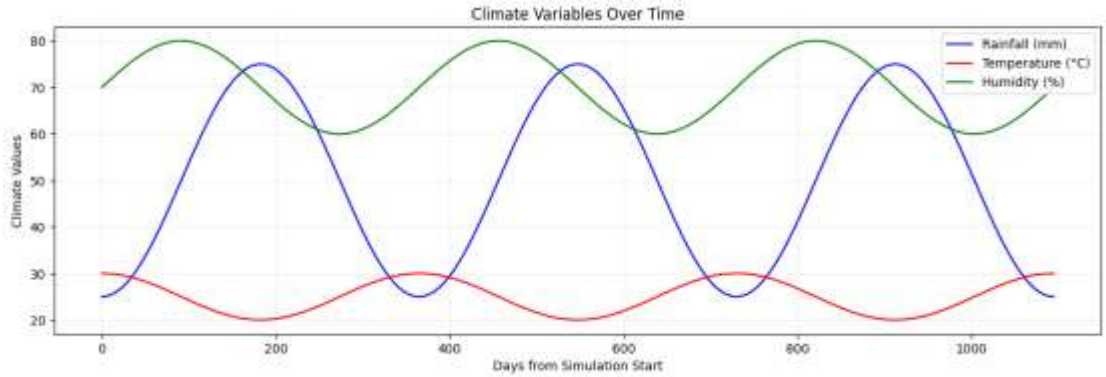


Fig4: Partial Rank Correlation Coefficients (PRCC)

These rankings imply that temperature-based early-warning thresholds should be prioritised in surveillance systems, while rainfall monitoring provides complementary predictive value, particularly during the monsoon season. The relatively modest contribution of humidity as a standalone driver suggests that its primary effect operates through its interaction with temperature rather than independently.

4.5 Disease-Specific Responses

Malaria transmission was sustained at humidity levels above 70% and temperatures in the range 22–28°C, with R_0 declining sharply above 30°C (Figure 5). This suppression is attributable to increased adult mosquito mortality at high temperatures, which shortens the infective lifespan of A. gambiae females. The longest simulated outbreaks occurred at 25–30°C with humidity exceeding 70%, conditions that characterise the wet season in many sub-Saharan and South Asian settings. Extreme heat events (>35°C) consistently shortened outbreak duration by increasing μ_v and reducing R_0 below unity.

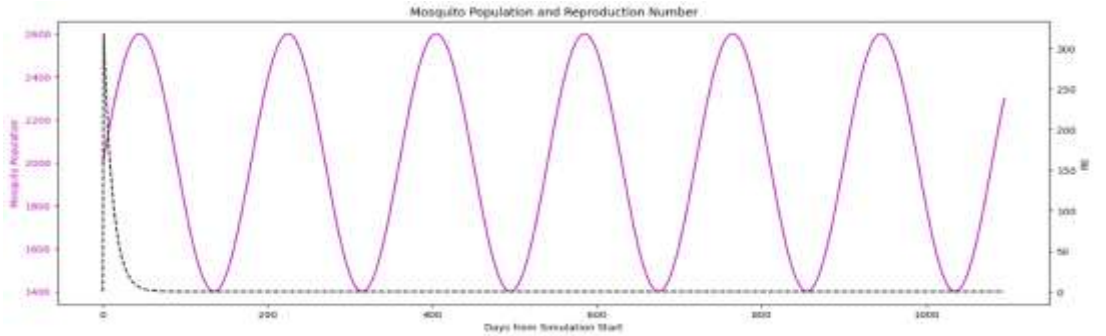


Fig5: Outbreak Duration vs. Humidity and Temperature

Dengue transmission was most intensive in the temperature range 25–32°C with moderate humidity (60–75%), particularly in high-urbanisation scenarios (U = 0.8; Figure 6). The coupled outbreak dynamics depicted in Figure 6 show that dengue and malaria seasonal peaks are partially offset—dengue peaking approximately three weeks later than malaria due to the higher thermal optimum of A. aegypti—with both peaks coinciding with the early post-monsoon period in South Asian settings. This temporal offset has practical implications for healthcare resource allocation.

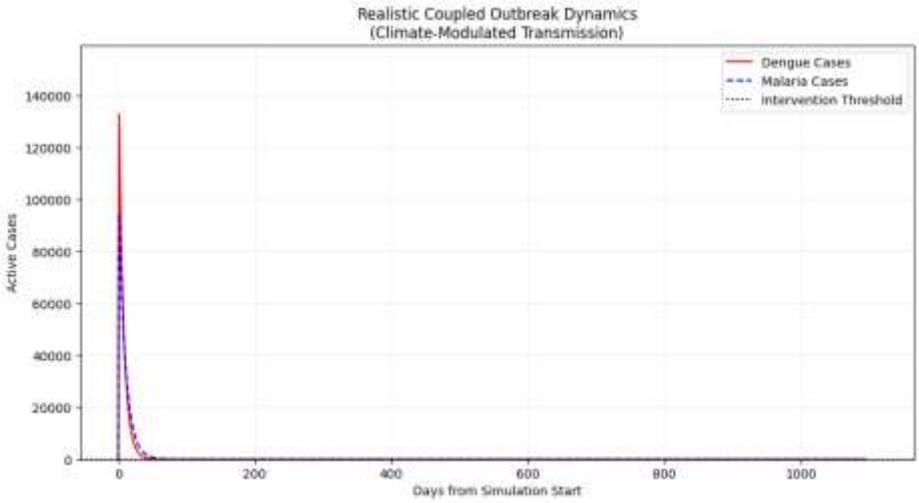


Fig6: Realistic Coupled Outbreak Dynamics

4.6 Policy Implications

The identification of a +2°C temperature threshold as a critical driver of outbreak probability transition supports the implementation of heat-triggered vector control protocols. Specifically, the model suggests that deploying larval source reduction and adult mosquito control measures when a 14-day rolling mean temperature anomaly exceeds +1.5°C above the seasonal climatological mean could intercept outbreak trajectories before exponential growth is established. Integration of R_0 estimates derived from near-real-time weather station data into national dengue and malaria early-warning systems represents a technically feasible and cost-effective application of the present framework.

5. Conclusion

This study has developed an analytically tractable, climate-sensitive SEIR-V compartmental model for dengue fever and malaria, incorporating temperature-, rainfall-, and humidity-dependent mosquito population functions derived from empirical thermal performance curves. The basic reproduction number R_0 was derived analytically using the next-generation matrix method, and local stability of the disease-free and endemic equilibria was established. Numerical simulations and PRCC-based sensitivity analysis quantified the relative contributions of climatic drivers to outbreak intensity and identified critical thresholds—notably a +2°C temperature anomaly and 80% relative humidity—beyond which epidemic potential increases nonlinearly.

Temperature emerged as the dominant climatic driver (PRCC = 0.75), followed by rainfall and humidity, with disease-specific thermal optima consistent with established empirical findings. The model also captured the temporal offset between dengue and malaria seasonal peaks in South Asian settings, providing a basis for coordinated surveillance and resource planning.

Future work should extend the model to include spatial heterogeneity through patch or partial differential equation formulations, incorporate age-structured human populations, and validate against multi-year surveillance data from high-burden districts in India. Coupling the model with regional climate model outputs under IPCC SSP scenarios would enable quantitative projections of long-term disease burden under alternative emission pathways.

References

[1] World Health Organization. (2023). Vector-borne diseases. WHO Fact Sheet. Geneva: WHO. Available at: https://www.who.int/news-room/fact-sheets/detail/vector-borne-diseases

[2] Bhatt, S., Gething, P.W., Brady, O.J., et al. (2013). The global distribution and burden of dengue. Nature, 496(7446), 504–507. https://doi.org/10.1038/nature12060

[3] World Health Organization. (2023). World Malaria Report 2023. Geneva: WHO. ISBN 978-92-4-008735-5.

[4] Mordecai, E.A., Cohen, J.M., Evans, M.V., et al. (2017). Detecting the impact of temperature on transmission of Zika, dengue, and chikungunya using mechanistic models. PLOS Neglected Tropical Diseases, 11(4), e0005568. https://doi.org/10.1371/journal.pntd.0005568

[5] Brady, O.J., Johansson, M.A., Guerra, C.A., et al. (2013). Modelling adult Aedes aegypti and Aedes albopictus survival at different temperatures in laboratory and field settings. Parasites & Vectors, 6(1), 351. https://doi.org/10.1186/1756-3305-6-351

[6] IPCC. (2021). Climate Change 2021: The Physical Science Basis. Contribution of Working Group I to the Sixth Assessment Report. Cambridge University Press. https://doi.org/10.1017/9781009157896

[7] Caminade, C., Kovats, S., Rocklov, J., et al. (2014). Impact of climate change on global malaria distribution. Proceedings of the National Academy of Sciences, 111(9), 3286–3291. https://doi.org/10.1073/pnas.1302089111

[8] Ryan, S.J., Carlson, C.J., Mordecai, E.A., & Johnson, L.R. (2019). Global expansion and redistribution of Aedes-borne virus transmission risk with climate change. PLOS Neglected Tropical Diseases, 13(3), e0007213.

[9] Paaijmans, K.P., Blanford, S., Bell, A.S., et al. (2010). Influence of climate on malaria transmission depends on daily temperature variation. Proceedings of the National Academy of Sciences, 107(34), 15135–15139.

[10] Gubler, D.J. (2002). Epidemic dengue/dengue hemorrhagic fever as a public health, social and economic problem in the 21st century. Trends in Microbiology, 10(2), 100–103.

[11] Chitnis, N., Hyman, J.M., & Cushing, J.M. (2008). Determining important parameters in the spread of malaria through the sensitivity analysis of a mathematical model. Bulletin of Mathematical Biology, 70(5), 1272–1296.

[12] Bhattacharya, S., Basu, P., & Bhattacharya, S. (2019). The yellow fever/dengue vector, Aedes aegypti, in the context of its ecology in the Indian subcontinent. Asian Pacific Journal of Tropical Disease, 9(1), 1–8.

[13] Ross, R. (1911). The Prevention of Malaria (2nd ed.). London: John Murray.

[14] Hoshen, M.B., & Morse, A.P. (2004). A weather-driven model of malaria transmission. Malaria Journal, 3, 32. https://doi.org/10.1186/1475-2875-3-32

[15] Wang, Y., et al. (2023). Impact of climate change on dengue fever epidemics in South and Southeast Asian settings: A modelling study. Infectious Disease Modelling, 8(3), 645–658. https://doi.org/10.1016/j.idm.2023.05.003

[16] Bonnin, L., Tran, A., Herbreteau, V., Marcombe, S., Boyer, S., Mangeas, M., & Menkes, C. (2022). Predicting the effects of climate change on dengue vector densities in Southeast Asia through process-based modelling. PLOS Neglected Tropical Diseases, 16(9), e0010666.

[17] Bal, S., & Sodoudi, S. (2020). Modeling and prediction of dengue occurrences in Kolkata, India, based on climate factors. International Journal of Biometeorology, 64(8), 1379–1391. https://doi.org/10.1007/s00484-020-01921-4

[18] Taghikhani, R., & Gumel, A.B. (2018). Mathematics of dengue transmission dynamics: Roles of vector vertical transmission and temperature fluctuations. Infectious Disease Modelling, 3, 266–292. https://doi.org/10.1016/j.idm.2018.09.003

[19] Brady, O.J., Golding, N., Pigott, D.M., et al. (2014). Global temperature constraints on Aedes aegypti and Ae. albopictus persistence and competence for dengue virus transmission. Parasites & Vectors, 7(1), 338.

[20] van den Driessche, P., & Watmough, J. (2002). Reproduction numbers and sub-threshold endemic equilibria for compartmental models of disease transmission. Mathematical Biosciences, 180(1–2), 29–48.

[21] Blower, S.M., & Dowlatabadi, H. (1994). Sensitivity and uncertainty analysis of complex models of disease transmission: an HIV model as an example. International Statistical Review, 62(2), 229–243.